

**SECURITY ASSESMENT AND ENHANCEMENT OF AN INTERCONNECTED POWER SYSTEM USING DIFFERENT FACTS DEVICES CONSIDERING VOLTAGE DEPENDENT LOADS AND ZIP LOADS**

**T. A. Ramesh Kumar**

Assistant Professor, Department of Electrical Engineering, Annamalai University, Chidambaram

**ABSTRACT**

*This paper has demonstrated the need for the proper remedial measures for security enhancement depending on system conditions, the dynamic behaviour of the reactive part of loads can be more significant than the real part. This paper had indicated that the dynamic load models will not only affect the damping of electromechanical modes, but can also have an influence on which generators participated in the mode. As load parameters vary, this participation can also vary. In this approach, with Voltage Depended Load (VDL) models and ZIP loads are considered for the quick restoration few FACTS devices are incorporated with boundary values. The security enhancement results are provided to highlight the overall security and suitability of the approach. The significant of the corrective measures to be adopted for the load uncertainty was also considered with load parameters variation. The proposed scheme is adopted in IEEE 14 bus test system. The optimized result can be utilized for the improvement of the system performance.*

*Keywords: Flexible AC Transmission System (FACTS), Interline Power Flow Controller (IPFC), Mixed Load and Thermostatically Controlled Loads*

**1. INTRODUCTION**

This paper proposes the control strategy for power system security assessment of an interconnected power system with Voltage Dependent Load (VDL) and ZIP Loads which is governed by the Flexible AC Transmission system (FACTS) controllers when the arrangement is impending an severe crisis state. First the islanding of the power system is avoided with the adoption the few FACTS devices. The scheme is adopted in test system of IEEE 14 bus using bacterial foraging optimization algorithm. The basic restoration assessment for the interconnected power system with Voltage Dependent Load (VDL)/ ZIP Loads has been conceded out and the various remedial control actions using few FACTS devices are considered for the power system security enhancement [1]. The maximum allowable limits are fixed if the system survives for all realistic contingencies or with reduced allowable limits by some small amount to provide a margin that would account for changes in conditions when the actual limit is in force.

**II. MATHEMATICAL MODELLING OF VOLTAGE DEPENDENT LOAD (VDL)**

Voltage Dependent Loads (VDL) represents the power relationship to voltage as an exponential equation of nonlinear load model. The load powers PH and QH are represented as negative powers as they are engrossed from the bus and are as follows [2]

$$-P_H = P_0 (v/v_0)^{\gamma_p} \tag{2.1}$$

$$-Q_H = Q_0 (v/v_0)^{\gamma_q} \tag{2.2}$$

Where  $v_0$  is the initial value of the load bus voltage obtained from power flow solution. Generally the exponent values of the model for different load components  $\gamma_p$  and  $\gamma_q$  are considered as (0, 1 or 2). Equations can be directly included in the formulation of power flow analysis. However, VDLs are generally initialized after the power flow analysis,  $P_0$  and  $Q_0$  are computed based on constant PQ load powers ( $P_{L0}$  and  $Q_{L0}$ ); In this case, the initial voltage is not known  $V_0$ , the subsequent equation can be used,

$$P = P_0 V^{\gamma_p} \tag{2.3}$$

$$Q = Q_0 V^{\gamma_q} \tag{2.4}$$

Where  $\gamma_p, \gamma_q$  are the active and reactive power exponents respectively.  $P_0$  and  $Q_0$  initial values of depend on the status parameter k. If  $k=1$ , after the power flow analysis the VDL is initialized and  $P_0, Q_0$  are denoted in percentage of the PQ load power allied at the VDL bus.

$$P_0 = \frac{k_p}{100} P_L \tag{2.5}$$

$$Q_0 = \frac{k_q}{100} P_L \tag{2.6}$$

**2.1 MATHEMATICAL MODELLING OF ZIP LOAD**

Polynomial or ZIP loads are the nonlinear load model whose powers are represented by the quadratic expression of the bus voltage. The ZIP model, equations (2.7) and (2.8), is a polynomial model that represents the sum of these three categories [3]

$$-P_H = g \left( \frac{v}{v_0} \right)^2 + I_p \frac{v}{v_0} + p_m \tag{2.7}$$

$$-q_H = b \left( \frac{v}{v_0} \right)^2 + I_q \frac{v}{v_0} + q_m \tag{2.8}$$

Where  $v_0$  is the initial voltage of the load bus and is obtained from the power flow solution. Other parameters of ZIP load is initialized after the power flow analysis [4] the parameters can be defined based on the PQ load powers  $P_{L0}$  and  $Q_{L0}$ .

$$g = \frac{g}{100} \frac{P_{L0}}{v_0^2}, \quad I_p = \frac{I_p}{100} \frac{P_{L0}}{v_0}, \quad p_m = \frac{p_m}{100} P_{L0}$$

$$b = \frac{b}{100} \frac{Q_{L0}}{v_0^2}, \quad I_q = \frac{I_q}{100} \frac{Q_{L0}}{v_0}, \quad q_m = \frac{q_m}{100} Q_{L0}$$

If the first voltage  $V_0$  not known, then the subsequent equations can be used

$$-P_H = g v^2 + I_p v + p_m \tag{2.9}$$

$$-q_H = b v^2 + I_q v + q_m \tag{2.10}$$

As the parameters are constants and indicate the nominal power they can be separated into constant impedance, constant current and constant power [5].

**III. IDENTIFICATION OF MODEL PARAMETERS.**

The real and reactive power representations of the model are

$$P_H = [1 + K_p(V - 1)](1 - P_{drop}) + P_{dyn} (G.V^2 - 1) \tag{2.11}$$

$$Q_H = [1 + K_q(V - 1)](1 - Q_{drop}) + Q_{dyn} (B.V^2 - 1) \tag{2.12}$$

Considering the equation (2.11), using re-parameterization the nonlinear relationship between P (active power), V (voltage at the load bus), G (conductance) and the parameters  $P_{dyn}$ ,  $P_{drop}$  and  $K_p$ , and the model can be written as (2.13).

$$P_H = [x(1) + x(2).(V - 1)] + P_{dyn} .(G.V^2 - 1) \tag{2.13}$$

$$x(1) = (1 - P_{drop}) \tag{2.14}$$

$$x(2) = x(1).K_p \tag{2.15}$$

$$z(t) = \gamma^t(t)\theta_p \tag{2.16}$$

$$\theta_p = (x(1), x(2), P_{dyn}) \tag{2.17}$$

The least squares method is used [6] to diminish the function (2.17) and to get the most excellent estimate for the parameter vector  $\theta_p$ .

$$L(\theta_p) = \sum_{k=1}^N \left( P_{simulated}(t_k, \theta_p) - P_{measured}(t_k, \theta_p) \right)^2 \tag{2.18}$$

The same procedure is applied for the reactive power also. The nonlinear model parameters can also be estimated accurately by an iterative approach as mentioned below, Initial estimate  $x_o$  for the parameters is selected. Best estimates are compared with the initial estimates to decide for further improvement [7].

**IV.COMPUTATION OF VOLTAGE COLLAPSE PERFORMANCE INDICES (VCPI)**

With the power flow model, Jacobian Matrix J represents the first derivatives of active and reactive power mismatch equations,  $\Delta P = \Delta P(\theta, E)$  and  $\Delta Q = \Delta Q(\theta, E)$ , with respect to the voltage magnitude E and angles  $\theta$ , i.e., the linearization of these equations yields

$$\begin{bmatrix} \Delta P \\ \Delta Q \end{bmatrix} = J \begin{bmatrix} \Delta \theta \\ \Delta E \end{bmatrix} \tag{4.42}$$

Where  $[\Delta P]$ ,  $[\Delta Q]$ ,  $[\Delta \theta]$  and  $[\Delta E]$  are the increments change in nodal bus powers, reactive power, angles and voltage magnitudes.

$$[J] = \begin{bmatrix} J_1 & J_2 \\ J_3 & J_4 \end{bmatrix} \tag{2.19}$$

$$J_1 = \frac{\partial P}{\partial \theta}, \quad J_2 = \frac{\partial P}{\partial E}, \quad J_3 = \frac{\partial Q}{\partial \theta}, \quad J_4 = \frac{\partial Q}{\partial E} \tag{2.20}$$

The voltage stability of the system is affected by both P and Q. However, at each operation point we keep P constant and evaluate voltage stability by considering the incremental relationship between Q and ( E or V ). This is analogous to the Q-V curve approach. In [8], the authors proposed to reduce the load-flow Jacobian to the first derivative of reactive power equations in relation to voltage magnitude, by assuming that the generator and load buses present no active power variation, i.e.,  $\Delta P = 0$ . Thus,

$$\begin{bmatrix} \Delta P \\ \Delta Q \end{bmatrix} = \begin{bmatrix} J_1 & J_2 \\ J_3 & J_4 \end{bmatrix} \begin{bmatrix} \Delta \theta \\ \Delta E \end{bmatrix} \tag{4.45}$$

$$[\Delta \theta] = -[J_{P\theta}]^{-1} \cdot [J_{PE}] \cdot [\Delta E] \tag{2.21}$$

$$[\Delta Q] = [J_{Q\theta}] [\Delta \theta] + [J_{QE}] \cdot [\Delta E] \tag{2.22}$$

After substituting  $[\Delta \theta]$ ,  $[\Delta Q]$

$$[\Delta Q] = \left( [J_{QE}] - [J_{Q\theta}] \cdot [J_{P\theta}]^{-1} \cdot [J_{PE}] \right) \cdot [\Delta E] \tag{2.23}$$

or

$$[\Delta Q]_{load} = [J] \cdot [R] \cdot [\Delta E]_{load} \tag{2.24}$$

$$\Delta Q = \left( J_4 - J_3 J_1^{-1} J_2 \right) \Delta E = JR \Delta E \tag{2.25}$$

Where

$$[J] \cdot [R] = \left( [J_{QE}] - [J_{Q\theta}] \cdot [J_{P\theta}]^{-1} \cdot [J_{PE}] \right) \tag{2.26}$$

$$[\Delta V]_{load} = [J] \cdot [R]^{-1} \cdot [\Delta Q]_{load} \tag{2.27}$$

$$\Delta E = \left( J_4 - J_3 J_1^{-1} J_2 \right)^{-1} \Delta Q = J R^{-1} \Delta Q \tag{2.28}$$

Where  $[J][R]^{-1}$  is called inverse reduced V-Q Jacobian matrix. Its  $i^{\text{th}}$  diagonal element is the V-Q sensitivity at the bus  $i$ .

Few parameters can be directly measured and can be used in real time application to compute proximity to collapse index quickly. An example of such indicator is sensitivity of the generated reactive powers with respect to load parameters and voltage magnitude. Voltage Collapse Performance Index (VCPI) is obtained using sensitivity analysis computation using the relation between voltage change and reactive power change and the elements of the inverse of the reduced Jacobian matrix  $JR$  are Q-V sensitivities [9]. The diagonal components  $\partial V_i / \partial Q_i$  are the self sensitivities and the nondiagonal elements  $\partial E_k / \partial Q_i$  are the mutual sensitivities. The sensitivities of voltage controlled buses are equal to zero. For a quite stable system when Q decreases at specified bus or buses [10], its effect on the voltage magnitude of the system buses should be minor. The sensitivity indices are interpreted as follows:

*Positive sensitivities:* Stable operation; the smaller the sensitivity, the more stable the system. As stability decreases, the magnitude of the sensitivity increases, becoming infinite at the stability limit (maximum loadability).

*Negative sensitivities:* Unstable operation. The system is not controllable, because all reactive power control devices are designed to operate satisfactorily when an increase in Q is accomplished by an increase in V.

**V. SIMULATION RESULTS AND OBSERVATIONS**

IEEE 14 bus system is considered for the Security Assessment studies. The performance analysis of IEEE 14-bus, 5-generator system coordinated with different types of Dynamic load models without and with FACTS devices were studied [11-17]. And the optimum utilization requirement with the FACTS devices for each load was determined using BFO technique [18-22]. In this case of study the buses 4, 5 and 14 are connected with VDL and ZIP Loads. The FACTS devise are connected as follows

1. SVC at Buses 4, 5 and 14.
2. UPFC between Buses 4 and 5, i.e. in Line 7.
3. UPFC between Buses 14 and 13, i.e. in Line 20.
4. IPFC between Buses 4 and 5, i.e. between Lines 7 and 9.
5. IPFC at Bus 14 i.e. in between Lines 17 and 20
6. IPFC at Bus 14 i.e. in between Lines 17 and 20

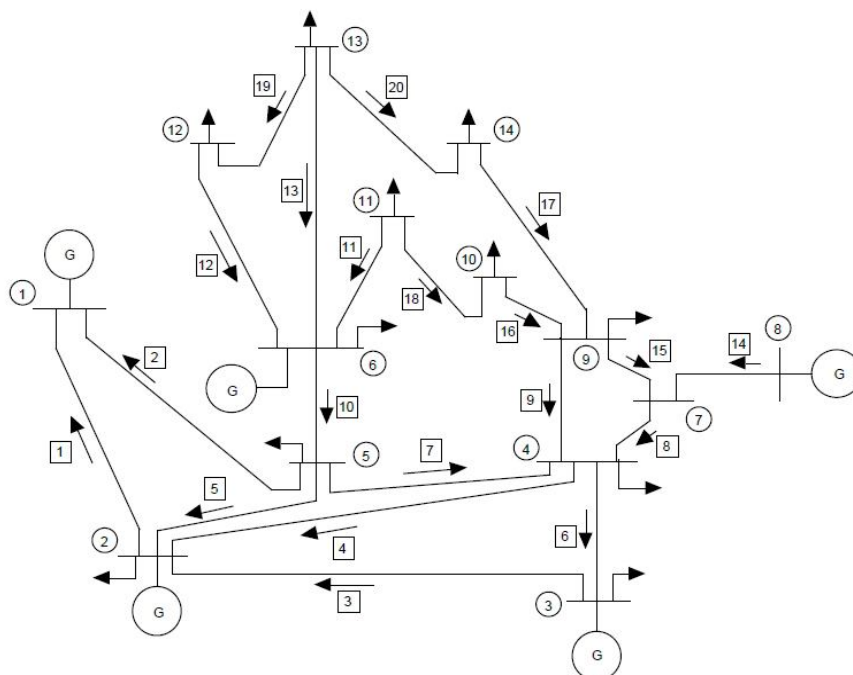


Fig-1: IEEE 14 Bus Systems

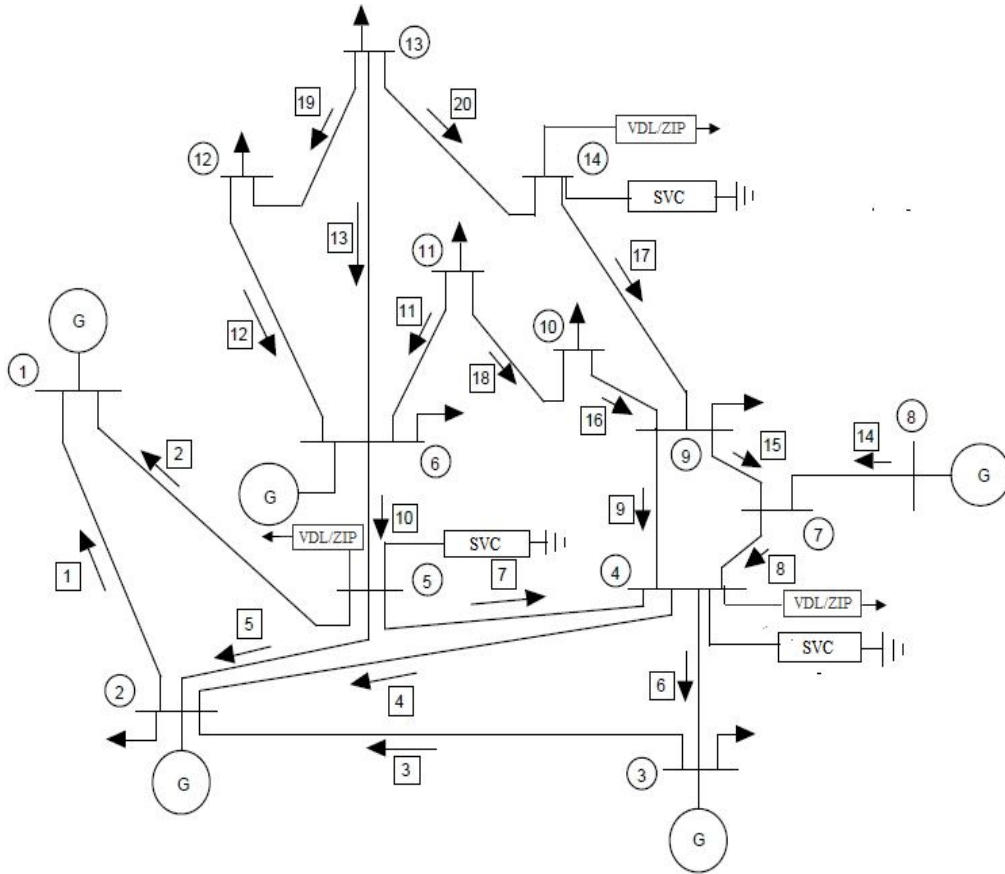


Fig-2: Single line diagram representation of IEEE 14 bus system with various SVC controllers

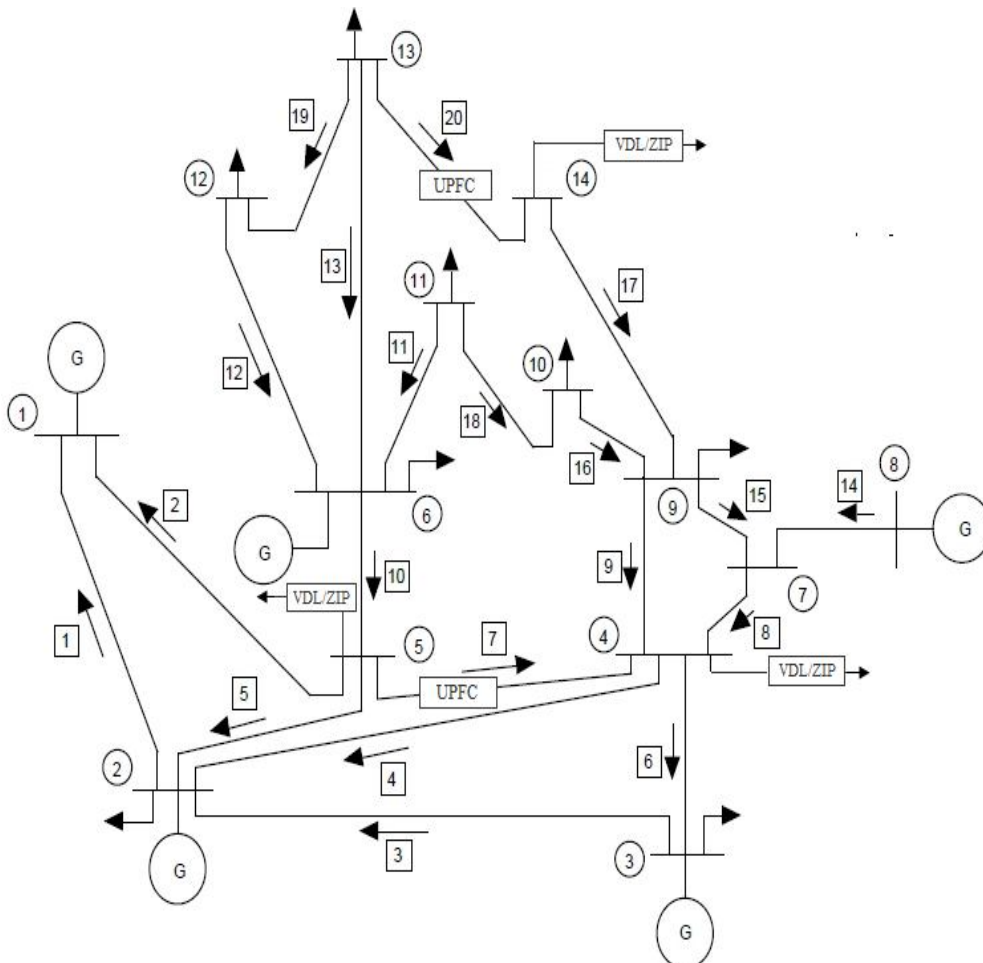


Fig-3: Single line diagram representation of IEEE 14 bus system with various UPFC controllers

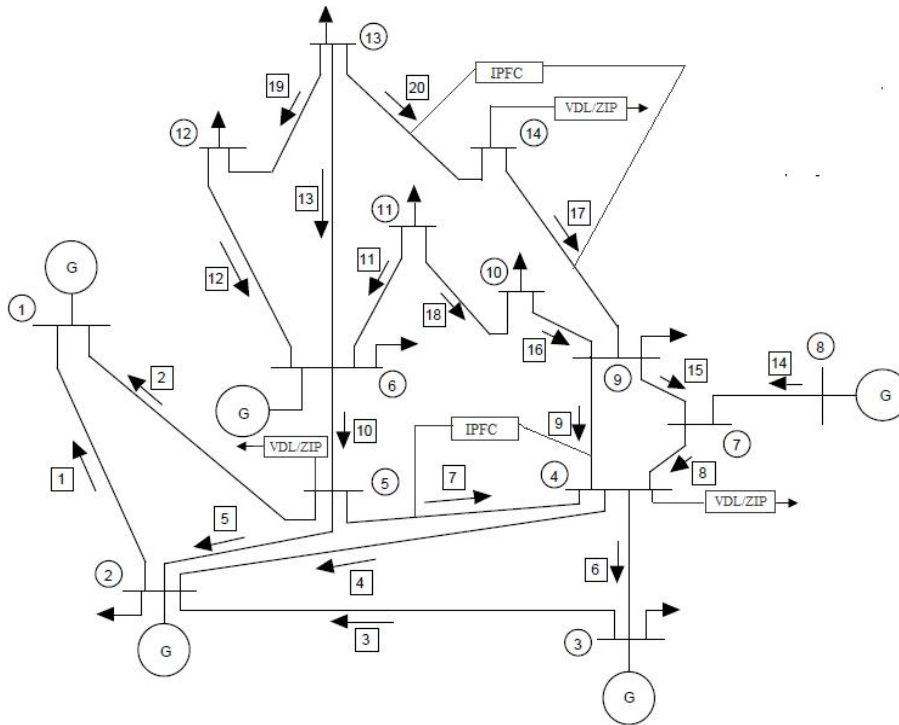


Fig-4: Single line diagram representation of IEEE 14 bus system with various IPFC controllers

Table-1: Power flow solution for IEEE 14 Bus systems with VDL Load in bus 4, 5 and bus 14

Bus No.	Voltage Magnitude	Voltage Angle	Real Power	Reactive Power
1	1.0000	0.0000	2.3485	-0.4328
2	1.0000	-5.899	0.1830	0.6521
3	0.9800	-14.668	-0.9420	0.3070
4	0.9608	-11.565	-0.4780	0.0390
5	0.9622	-9.888	-0.0760	-0.0160
6	1.000	-16.291	-0.1120	0.1050
7	0.9774	-14.960	0.0000	0.0000
8	1.0000	-14.959	0.0000	0.1283
9	0.9620	-16.784	-0.2950	-0.1660
10	0.9606	-17.023	-0.0900	-0.0580
11	0.9762	-16.793	-0.0350	-0.0180
12	0.9823	-17.269	-0.0610	-0.0160
13	0.9755	-17.317	-0.1350	-0.0580
14	0.9482	-18.202	-0.1490	-0.0500

Table-2: Weak bus identification using VCP indices with VDL Load

BUS	VCP INDICES
4	37.1684
5	34.1629
14	23.1737
7	19.0999
10	14.1190
13	10.3430
11	8.2745
12	5.3145
9	4.9980

**Table-3: Power flow solution for IEEE 14 Bus systems with VDL Load and SVC in bus 4**

Bus No.	Voltage Magnitude	Voltage Angle	Real Power	Reactive Power
1	1.0300	0.00	2.2681	-0.0643
2	1.0000	-5.402	0.2472	-0.0306
3	0.9900	-14.185	-0.9420	0.3035
4	0.9800	-11.352	-0.4780	0.0430
5	0.9764	-9.610	-0.0592	0.0232
6	1.0000	-15.935	-0.1120	-0.0151
7	0.9658	-14.733	0.0000	0.0000
8	1.0000	-14.732	0.0000	-0.0806
9	0.9698	-16.571	-0.2950	-0.1660
10	0.9671	-16.785	-0.0900	-0.0580
11	0.9795	-16.500	-0.0350	-0.0180
12	0.9827	-16.929	-0.0610	-0.0160
13	0.9762	-17.005	-0.1350	-0.0580
14	0.9513	-18.035	-0.1614	-0.0541

**Table-4: Power flow solution for IEEE 14 Bus systems with VDL Load and SVC in bus 5**

Bus No.	Voltage Magnitude	Voltage Angle	Real Power	Reactive Power
1	1.0300	- 0.000	2.2677	-0.0745
2	1.0000	-5.392	0.2472	-0.0557
3	0.9900	-14.200	-0.9420	0.3444
4	0.9731	-11.206	-0.4780	0.0390
5	0.9800	-9.650	-0.0591	0.0196
6	1.0000	-15.943	-0.1120	0.0153
7	0.9827	-14.631	0.00	0.0000
8	1.0000	-14.630	0.00	-0.0981
9	0.9669	-16.484	-0.2950	-0.1660
10	0.9647	-16.714	-0.0900	-0.0580
11	0.9783	-16.467	-0.0350	-0.0180
12	0.9825	-16.934	-0.0610	-0.0160
13	0.9758	-16.999	-0.1350	-0.0580
14	0.9495	-17.988	-0.1614	-0.0541

**Table-5: Power flow solution for IEEE 14 Bus systems with VDL Load and SVC in bus 14**

Bus No.	Voltage Magnitude	Voltage Angle	Real Power	Reactive Power
1	1.0300	0.000	2.2687	-0.0330
2	1.0000	-5.422	0.2473	-0.1385
3	0.9900	-14.290	-0.9420	0.3732
4	0.9670	-11.189	-0.4780	0.0390
5	0.9685	-9.508	-0.0594	0.0229
6	1.0000	-15.802	-0.1120	0.0251
7	0.9845	-14.656	0.0000	0.0000
8	1.0000	-14.656	0.0000	-0.0851
9	0.9741	-16.506	0.2950	-0.1660
10	0.9706	-16.712	-0.0900	-0.0580
11	0.9814	-16.409	-0.0350	-0.0180
12	0.9862	-16.864	-0.0610	-0.0160
13	0.9827	-17.070	-0.1350	-0.0580
14	0.9482	-18.202	-0.1490	-0.0500

**Table-6: Weak bus identification indices after incorporating SVC unit in bus 4, 5 and 14 in a IEEE 14 bus system with VDL Load**

BUS	VCP INDICES
4	36.7603
5	28.1737
14	20.4378
7	18.1071
10	13.4062
13	9.6290
11	7.8766
12	5.1158
9	4.8146

**Table-7: Power flow solution for IEEE 14 Bus systems with VDL Load and UPFC connected to the Bus 4 in line 7**

Bus No.	Voltage Magnitude	Voltage Angle	Real Power	Reactive Power
1	1.0300	0.000	2.2709	-0.0922
2	1.0000	-5.401	0.2472	-0.1086
3	1.0000	-14.249	-0.9420	0.3546
4	0.9900	-11.482	-0.4780	0.0437
5	0.9826	-9.678	-0.0590	0.0234
6	1.0000	-15.870	-0.1120	-0.0244
7	0.9900	-14.579	0.0000	0.0023
8	1.0000	-14.579	0.0000	-0.0568
9	0.9741	-16.488	-0.2950	-0.1660
10	0.9706	-16.7005	-0.0900	-0.0580
11	0.9814	-16.431	-0.0350	-0.0180
12	0.9831	-16.860	-0.0610	-0.0160
13	0.9768	-16.937	-0.1350	-0.0580
14	0.9541	-17.952	-0.1614	-0.0541

**Table-8: Power flow solution for IEEE 14 Bus systems with VDL Load and UPFC connected to the Bus 5 in line7**

Bus No.	Voltage Magnitude	Voltage Angle	Real Power	Reactive Power
1	1.0300	- 0.000	2.2689	-0.1180
2	1.0000	-5.366	0.2471	-0.1455
3	1.0000	-14.158	-0.9420	0.3548
4	0.9900	-11.341	-0.4780	0.0434
5	0.9900	-9.803	-0.0588	0.0201
6	1.0100	-15.960	-0.1120	0.0083
7	0.9920	-14.675	0.0000	0.0000
8	1.0000	-14.675	0.0000	-0.0455
9	0.9777	-16.490	-0.2950	-0.1660
10	0.9754	-16.716	-0.0900	-0.0580
11	0.9887	-16.474	-0.0350	-0.0180
12	0.9927	-16.931	-0.0610	-0.0160
13	0.9861	-16.995	-0.1350	-0.0580
14	0.9603	-17.962	-0.1614	-0.0541

**Table-9: Power flow solution for IEEE 14 Bus systems with VDL Load and UPFC connected to the Bus 14 in line 20**

Bus No.	Voltage Magnitude	Voltage Angle	Real Power	Reactive Power
1	1.0300	0.000	2.2689	-0.0426
2	1.0000	-5.416	0.2472	-0.1151
3	0.9900	-14.267	-0.9420	0.3621
4	0.9688	-11.201	-0.4780	0.0390
5	0.9707	-9.541	-0.0593	0.0230
6	0.0100	-15.845	-0.1120	0.0402
7	0.9847	-14.618	0.0000	0.0000
8	1.0000	-14.618	0.0000	-0.0685
9	0.9793	-16.435	0.2950	-0.1660
10	0.9768	-16.650	-0.0900	-0.0580
11	0.9894	-16.385	-0.0350	-0.0180
12	0.9949	-16.855	-0.0610	-0.0160
13	0.9900	-17.009	-0.1350	-0.0575
14	0.9900	-18.604	-0.1614	-0.0526

**Table-10: Weak bus identification indices after incorporating UPFC unit in Line 7 and 20 in a IEEE 14 Bus system with VDL Load**

BUS	VCP INDICES
4	32.9007
5	24.2566
14	16.7444
7	14.7694
10	9.4875
13	5.6394
11	3.8012
12	1.0973
9	0.9985

**Table-11: Power flow solution for IEEE 14 Bus systems with VDL Load and IPFC Between lines 9 and 7 at bus 4**

Bus No.	Voltage Magnitude	Voltage Angle	Real Power	Reactive Power
1	1.0300	0.000	2.2707	-0.1619
2	1.0000	-5.351	0.2471	-0.2584
3	1.0000	-14.082	-0.9420	0.2953
4	1.0000	-11.466	-0.4780	0.0438
5	1.0000	-9.925	-0.0586	0.0209
6	1.0100	-15.891	-0.1120	-0.0559
7	1.0000	-14.547	0.0000	0.0023
8	1.0000	-14.546	0.0000	-0.0000
9	0.9845	-16.416	-0.2950	-0.1660
10	0.9810	-16.643	-0.0900	-0.0580
11	0.9916	-16.407	-0.0350	-0.0180
12	0.9932	-16.855	-0.0610	-0.0160
13	0.9871	-16.926	-0.1350	-0.0580
14	0.9647	-17.879	-0.1614	-0.0541

**Table-12: Power flow solution for IEEE 14 Bus systems with VDL Load and IPFC Between lines 9 and 7 at bus 5**

Bus No.	Voltage Magnitude	Voltage Angle	Real Power	Reactive Power
1	1.0300	- 0.000	2.2696	-0.1618
2	1.0000	-5.349	0.2471	-0.2586
3	1.0000	-14.080	-0.9420	0.2953
4	1.0000	-11.464	-0.4780	0.0438
5	1.0000	-9.918	-0.0586	0.0209
6	1.0200	-15.787	-0.1120	0.0365
7	1.0049	-14.671	0.0000	0.0000
8	1.0000	-14.671	0.0000	-0.0278
9	1.0000	-16.395	-0.2950	-0.1611
10	0.9957	-16.602	-0.0900	-0.0580
11	1.0041	-16.335	-0.0350	-0.0180
12	1.0038	-16.734	-0.0610	-0.0160
13	0.9981	-16.841	-0.1350	-0.0580
14	0.9785	-17.785	-0.1614	-0.0541

**Table-13: Power flow solution for IEEE 14 Bus systems with VDL Load and IPFC Between lines 17 and 20 at bus 14**

Bus No.	Voltage Magnitude	Voltage Angle	Real Power	Reactive Power
1	1.0300	0.000	2.2669	-0.0589
2	1.0000	-5.404	0.2472	-0.0696
3	0.9900	-14.228	-0.9420	0.3373
4	0.9731	-11.250	-0.4780	0.0390
5	0.9745	-9.573	-0.0592	0.0231
6	1.0200	-15.686	-0.1120	0.0459
7	0.9981	-14.661	0.0000	0.0000
8	1.0000	-14.661	0.0000	-0.0090
9	1.0000	-16.445	0.2950	-0.1604
10	0.9957	-16.625	-0.0900	-0.0580
11	1.0040	-16.297	-0.0350	-0.0180
12	1.0048	-16.656	-0.0610	-0.0164
13	1.0000	-16.783	-0.1350	-0.0578
14	1.0000	-18.231	-0.1614	-0.0530

**Table 14: Weak bus identification indices after incorporating IPFC unit in Lines 7, 9, 17 and 20 in an IEEE 14 Bus system with VDL Load**

BUS	VCP INDICES
4	30.8309
5	22.2802
14	11.1702
7	9.1742
10	8.8010
13	5.6075
11	3.7335
12	0.8957
9	0.8166

**Table-15: Power flow solution for IEEE 14 Bus systems with ZIP Load in bus 4, 5 and bus 14**

Bus No.	Voltage Magnitude	Voltage Angle	Real Power	Reactive Power
1	1.0300	0.0000	2.3630	-0.4339
2	1.0000	-5.385	0.1830	0.6576
3	0.9800	-14.727	-0.9420	0.3087
4	0.9605	-11.637	-0.4780	0.0390
5	0.9619	-9.956	-0.0790	0.0168
6	1.0000	-16.446	-0.1120	0.1105
7	0.9770	-15.090	0.0000	0.0000
8	1.0000	-15.890	0.0000	0.1304
9	0.9614	-16.945	-0.2950	-0.1660
10	0.9601	-17.182	-0.0900	-0.0580
11	0.9760	-16.950	-0.0350	-0.0180
12	0.9821	-17.438	-0.0610	-0.0152
13	0.9750	-17.496	-0.1350	-0.0580
14	0.9393	-30.181	-0.3521	0.0129

**Table-16: Weak bus identification index with its percentage before and after incorporating FACTS in IEEE 14 Bus system with VDL Load**

Bus No.	VCP Index							
	Without FACTS		SVC		UPFC		IPFC	
	Actual	%	Actual	%	Actual	%	Actual	%
<b>4</b>	37.16	<b>100</b>	36.76	<b>98.87</b>	32.90	<b>88.48</b>	30.83	<b>82.92</b>
<b>5</b>	34.16	<b>100</b>	28.17	<b>82.46</b>	24.25	<b>70.98</b>	22.28	<b>65.22</b>
<b>14</b>	23.17	<b>100</b>	20.43	<b>88.14</b>	11.74	<b>72.196</b>	11.17	<b>48.174</b>

**Table-17: Weak bus identification using VCP indices with ZIP Load**

BUS	VCP INDICES
4	37.1803
5	34.1731
14	23.1878
7	19.1071
10	14.1262
13	10.3490
11	8.2766
12	5.3158
9	5.0146

**Table-18: Power flow solution for IEEE 14 Bus systems with ZIP Load and SVC in bus 4**

Bus No.	Voltage Magnitude	Voltage Angle	Real Power	Reactive Power
1	1.0300	0.00	2.4962	0.1418
2	1.0000	-8.71	0.2289	-0.1436
3	1.9900	-21.73	-1.0362	0.3428
4	1.9800	-18.16	-0.5258	0.0486
5	0.9736	-15.48	-0.0652	0.0208
6	1.0000	-26.27	-0.1232	0.0390
7	0.9841	-24.24	0.0000	0.0000
8	1.0000	-24.23	0.0000	-0.0930
9	0.9675	-27.55	-0.3245	-0.1826
10	0.9642	-27.79	-0.0990	-0.0638
11	0.9777	-27.23	-0.0385	-0.0198
12	0.9806	-28.08	-0.0671	-0.0176
13	0.9711	-28.58	0.1485	0.0638
14	0.9392	-32.89	-0.3873	0.0142

**Table-19: Power flow solution for IEEE 14 Bus systems with ZIP Load and SVC in bus 5.**

Bus No.	Voltage Magnitude	Voltage Angle	Real Power	Reactive Power
1	1.0300	0.00	2.4992	-0.1632
2	1.0000	-8.68	0.2288	-0.2244
3	0.9800	-21.60	-1.0362	0.3005
4	0.9687	-17.87	-0.5258	0.0429
5	0.9800	-15.58	-0.0651	0.0173
6	1.0000	-26.30	-0.1232	0.0339
7	0.9790	-24.06	0.0000	0.0000
8	1.0000	-24.06	0.0000	0.1193
9	0.9626	-27.40	-0.3245	-0.1826
10	0.9603	-27.68	0.0990	-0.0638
11	0.9756	-27.19	-0.0385	-0.0198
12	0.9803	-28.11	-0.0671	-0.0176
13	0.9704	-28.60	-0.1485	-0.0638
14	0.9361	-32.84	-0.3873	0.0142

**Table-20: Power flow solution for IEEE 14 Bus systems with ZIP Load and SVC in bus 14**

Bus No.	Voltage Magnitude	Voltage Angle	Real Power	Reactive Power
1	1.0300	0.00	2.4993	-0.0941
2	1.0000	-8.75	0.2290	0.3640
3	0.9988	-21.80	-0.0362	0.3488
4	0.9592	-17.86	-0.5258	0.0429
5	0.9619	-15.33	-0.0655	0.0204
6	1.0100	-26.19	-0.1232	0.0651
7	0.9820	-24.09	0.0000	0.0000
8	1.0000	-24.09	0.0000	-0.0995
9	0.9741	-27.38	0.3245	-0.1826
10	0.9716	-27.63	-0.0990	-0.0638
11	0.9863	-27.10	-0.0385	-0.0198
12	0.9945	-28.05	-0.0671	-0.0176
13	0.9881	-28.73	-0.1485	-0.0638
14	0.9800	-33.67	-0.3873	0.0181

**Table-21: Weak bus identification indices after incorporating SVC unit in bus 4, 5 and 14 in a IEEE 14 bus system with ZIP Load**

BUS	VCP INDICES
4	35.6802
5	31.8207
14	29.7509
7	15.7071
10	13.5262
13	9.7490
11	7.8766
12	5.0158
9	4.7146

**Table 22: Power flow solution for IEEE 14 Bus systems with ZIP Load and UPFC connected to the Bus 4 in line 7**

Bus No.	Voltage Magnitude	Voltage Angle	Real Power	Reactive Power
1	1.0300	0.00	2.4962	0.1699
2	1.0000	-8.72	0.2289	-0.0047
3	1.0000	-21.89	-0.0362	0.3941
4	0.9900	-18.32	-0.5258	0.0495
5	0.9799	-15.55	-0.0651	0.0210
6	1.0000	-26.09	-0.1232	0.0047

7	0.9900	-23.92	0.0000	0.0035
8	1.0000	-23.92	0.0000	-0.0568
9	0.9729	-27.32	-0.3245	-0.1826
10	0.9668	-27.57	-0.0990	-0.0638
11	0.9800	-27.04	-0.0385	-0.0198
12	0.9811	-27.90	-0.0671	-0.0176
13	0.9720	-28.40	0.1485	0.0638
14	0.9428	-32.64	-0.3873	0.0142

Table-23: Power flow solution for IEEE 14 Bus systems with ZIP Load and UPFC connected to the Bus 5 in line7

Bus No.	Voltage Magnitude	Voltage Angle	Real Power	Reactive Power
1	1.0300	0.00	2.4992	-0.1935
2	1.0000	-7.98	0.0939	-0.3405
3	1.0000	-20.97	-1.0362	0.3942
4	0.9900	-17.40	-0.5258	0.0488
5	0.9900	-15.07	-0.0651	0.0604
6	1.0100	-25.54	-0.1232	0.0195
7	0.9903	-23.39	0.0000	0.0000
8	1.0000	-23.39	0.0000	-0.0549
9	0.9754	-26.65	-0.3245	-0.1826
10	0.9727	-26.91	0.0990	-0.0638
11	0.9869	-26.42	-0.0385	-0.0198
12	0.9907	-27.31	-0.0671	-0.0176
13	0.9811	-27.79	-0.1485	-0.0638
14	0.9484	-31.94	-0.3873	0.0142

Table-24: Power flow solution for IEEE 14 Bus systems with ZIP Load and UPFC connected to the Bus 14 in line 20

Bus No.	Voltage Magnitude	Voltage Angle	Real Power	Reactive Power
1	1.0300	0.00	2.4993	-0.0956
2	1.0000	-8.75	0.2290	0.3601
3	0.9800	-21.89	-0.0362	0.3460
4	0.9596	-17.89	-0.5258	0.0429
5	0.9622	-15.35	-0.0655	0.0204
6	1.0100	-26.21	-0.1232	0.0387
7	0.9835	-24.11	0.0000	0.0000
8	1.0000	-24.11	0.0000	-0.0905
9	0.9733	-27.39	0.3245	-0.1826
10	0.9742	-27.64	-0.0990	-0.0638
11	0.9877	-27.12	-0.0385	-0.0198
12	0.9955	-28.11	-0.0671	-0.0176
13	0.9900	-28.85	-0.1485	-0.0628
14	0.9900	-33.80	-0.3873	0.0184

Table-25: Weak bus identification indices after incorporating UPFC unit in Line 7 and 20 in a IEEE 14 Bus system with ZIP Load

BUS	VCP INDICES
4	27.6731
5	23.7566
14	21.7802
7	12.3694
10	9.6075
13	5.7594
11	3.8012
12	0.9973
9	0.8985

**Table-26: Power flow solution for IEEE 14 Bus systems with ZIP Load and IPFC Between lines 9 and 7 at bus 4**

Bus No.	Voltage Magnitude	Voltage Angle	Real Power	Reactive Power
1	1.0300	0.00	2.4962	0.1645
2	1.0000	-7.64	0.2485	-0.1779
3	1.0000	-19.42	-0.9420	0.2944
4	1.0000	-16.49	-0.4780	0.0452
5	0.9906	-14.04	-0.058	0.0234
6	1.0300	-23.43	-0.1120	0.0051
7	1.0042	-21.74	0.0000	0.0000
8	1.0000	-21.74	0.0000	-0.0239
9	0.9993	-24.56	-0.2950	-0.1660
10	0.9968	-24.76	-0.0900	-0.0580
11	1.0095	-24.27	-0.0350	-0.0180
12	1.0159	-25.05	-0.0610	-0.0160
13	1.0099	-25.62	0.1350	0.0580
14	1.0000	-29.83	-0.3521	0.0160

**Table-27: Power flow solution for IEEE 14 Bus systems with ZIP Load and IPFC Between lines 9 and 7 at bus 5**

Bus No.	Voltage Magnitude	Voltage Angle	Real Power	Reactive Power
1	1.0300	0.00	2.4992	-0.1703
2	1.0000	-7.68	0.2486	-0.2084
3	1.0000	-19.31	0.9420	0.2946
4	1.0000	-16.22	-0.4780	0.0450
5	1.0000	-13.94	-0.0581	0.0234
6	1.0400	-23.65	-0.1120	0.0150
7	1.0049	-21.26	0.0000	0.0055
8	1.0000	-21.26	0.0000	-0.0276
9	1.0005	-21.26	-0.2950	-0.1660
10	0.9997	-24.29	0.0900	-0.0580
11	1.0160	-24.13	-0.0350	-0.0180
12	1.0283	-25.43	-0.0610	-0.0160
13	1.0236	-26.26	-0.1350	-0.0580
14	1.0000	-28.34	-0.3521	0.0154

**Table-28: Power flow solution for IEEE 14 Bus systems with ZIP Load and IPFC Between lines 17 and 20 at bus 14**

Bus No.	Voltage Magnitude	Voltage Angle	Real Power	Reactive Power
1	1.0300	0.00	2.4993	0.1739
2	1.0000	-7.67	0.2486	0.2138
3	1.0000	19.28	-0.9420	0.2947
4	1.0000	-16.18	-0.4780	0.0449
5	0.9924	-13.97	-0.0581	0.0235
6	1.0500	-23.94	-0.1120	0.02162
7	1.0055	-21.02	0.0000	0.0000
8	1.0000	-21.02	0.0000	-0.0313
9	1.0018	-23.61	0.2950	-0.1660
10	1.0026	-24.05	-0.0900	-0.0580
11	1.0224	-24.14	-0.0350	-0.0180
12	1.0412	-25.86	-0.0610	-0.0160
13	1.0384	-26.92	-0.1350	-0.0580
14	1.0000	-27.26	-0.3521	0.0137

**Table-29: Weak bus identification indices after incorporating IPFC unit in Lines 7, 9, 17 and 20 in an IEEE 14 Bus system with ZIP Load**

BUS	VCP INDICES
4	20.5878
5	16.8944
14	11.3220
7	9.7742
10	8.9210
13	5.7275
11	3.7335
12	0.7957
9	0.7166

**Table-30: Weak bus identification indices with its percentage before and after incorporating FACTS in IEEE 14 Bus system with ZIP Load**

Bus No.	Without FACTS		SVC		UPFC		IPFC	
	Actual	%	Actual	%	Actual	%	Actual	%
<b>4</b>	37.02	<b>100</b>	33.88	<b>91.51</b>	30.02	<b>81.09</b>	27.95	<b>75.49</b>
<b>5</b>	34.03	<b>100</b>	27.67	<b>81.31</b>	23.75	<b>69.79</b>	21.78	<b>64.02</b>
<b>14</b>	23.17	<b>100</b>	20.58	<b>88.82</b>	16.89	<b>72.89</b>	11.32	<b>48.85</b>

## V. CONCLUSION

This paper deals with the coordinated emergency control with the usage of various FACTS devices especially SVC, UPFC, IPFC units. A method is needed to rapidly re-balance the power by either shedding some loads to maintain power flow to the remaining loads or directing the power flow across transmission corridors with greater capacity. In this study, Bacterial Foraging optimization (BFO) technique was adopted to ensure the stability of the system with various types of loads. Using the BFO algorithm the FACTS devices are turned to ensure sufficient power flow capacity so as to meet out the load effectively if the network is reconfigured to bypass the loss in the transmission capability. By adjusting the magnitude and phase angle of the series voltage source, the apparent impedance of the transmission line may be varied. This change in impedance may be translated into a similar change in maximum power flow capacity across the line. If the load cannot be served under the current operating scenario, then the BFO algorithm is used to solve by determining the minimum number of line capacity changes (implemented by the FACTS devices) that are required to continue to satisfy the load. It can be concluded that BFO technique can be easily adopted in ensuring an effective optimization technique in searching the optimum value of real and reactive power loading. It has been found that with the UPFC, IPFC controller, the risk of load shedding is considerably reduced and can easily be adopted for emergency control. From the results it has been found that the FACTS devices especially UPFC and IPFC successfully prevent the system from blackout and restore the system faster. The result points out that the FACTS devices parameter influence on the power system stability limits even though is negligible, it should be verified when other type of optimized technique are employed to the power system network.

## VI. ACKNOWLEDGEMENT

The authors wish to thank the authorities of Annamalai University, Annamalainagar, Tamilnadu, India for the facilities provided to prepare this paper.

## REFERENCES

1. J. Srivani and K.S. Swarup, "Power system static security assessment and evaluation using external system equivalents", *Electrical Power and Energy Systems*, Vol. 30, pp 83–92, 2008.
2. Dissanayaka.A, Annakkage.U.D, B. Jayasekara and B.Bagen, "Risk-Based Dynamic Security Assessment", *IEEE Transactions on Power Systems*, Vol. 26, No. 3, pp 1302-1308, 2011.
3. T. J. Overbye, "A Power Flow Measure for Unsolvable Cases", *IEEE Transactions on Power Systems*, Vol. 9, No. 3, pp. 1359–1365, 1994.
4. E. Handschin and D. Karlsson, "Nonlinear dynamic load modelling: model and parameter estimation," *IEEE Transactions on Power Systems*, Vol. 11, pp. 1689-1697, 1996.
5. J.V. Milanovic and I.A. Hiskens, "The effect of dynamic load on steady state stability of synchronous generator", *Proceedings in International conference on Electric Machines ICEM'94*, Paris, France, pp.154-162, 1994.

6. W Xu and Y. Mansour, "Voltage stability analysis using generic dynamic load models", IEEE Transaction Power system, Vol. 9, No.1, pp. 479-493, 1994.
7. D.Karlsson and D.J.Hill, "Modelling and identification of non-linear dynamic load in power systems", IEEE Transactions on Power Systems, Vol.9, No. 1, pp. 157-166, 1994.
8. S.A.Y. Sabir and D.C. Lee, "Dynamic load models derived from data acquired during system transients", IEEE Transactions on Power Apparatus and system, Vol. 101, No.9, pp. 3365-3372, 1982.
9. Y. Liang, R. Fischl, A. DeVito and S.C. Readinger, "Dynamic reactive load model", IEEE Transactions on Power Systems, Vol.13, No.4, pp.1365-1372, 1998.
10. E. Vaahedi, H. El-Din, and W. Price, "Dynamic load modelling in large scale stability studies", IEEE Transactions on Power Systems, Vol. 3, No. 3, pp. 1039-1045, 1988.
11. Xiao, Y., Song, Y.H., Liu, C.C. and Sun, Y.Z., "Available transfer capability enhancement using FACTS devices", IEEE Transactions on Power Systems, Vol. 18, No. 1, pp.305-312, 2003.
12. A.V. Naresh Babu and S. Sivanagaraju, "Assessment of Available Transfer Capability for Power System Network with Multi-Line FACTS Device", International Journal of Electrical Engineering, Vol .5, No. 1, pp. 71-78, 2012.
13. M. A. Abido," Power System Stability Enhancement Using FACTS Controllers: A Review", The Arabian Journal for Science and Engineering, Vol. 34, No 1B, pp 153-172, 2009.
14. Jianhong Chen, Tjing T. Lie, and D.M. Vilathgamuwa, "Basic control of interline power flow controller", Proc. of IEEE Power Engineering Society Winter Meeting, New York, USA, Jan. 27-31, pp.521-525, 2002.
15. Y. Zhang, C. Chen, and Y. Zhang, "A Novel Power Injection Model of IPFC for Power Flow Analysis Inclusive of Practical Constraints", IEEE Transactions on Power Systems, Vol. 21, No. 4, pp. 1550 – 1556, 2006.
16. S. Bhowmick, B. Das and N. Kumar, " An Advanced IPFC Model to Reuse Newton Power Flow Codes", IEEE Transactions on Power Systems, Vol. 24 , No. 2 , pp. 525- 532, 2009.
17. A.M. Shan Jiang, U.D. Gole Annakkage and D.A. Jacobson, "Damping Performance Analysis of IPFC and UPFC Controllers Using Validated Small-Signal Models", IEEE Transactions on Power Systems, Vol. 26, No. 1 , pp. 446- 454, 2011.
18. Babu, A.V.N and Sivanagaraju, S, "Mathematical modelling, analysis and effects of Interline Power Flow Controller (IPFC) parameters in power flow studies", IEEE Transactions on Power Systems, Vol. 19, pp. 1-7, 2011.
19. Tang, W.J. Li, M.S. Wu, Q.H. Saunders, J.R. , " Bacterial Foraging Algorithm for Optimal Power Flow in Dynamic Environments", IEEE Transactions on Power Systems, Vol. 55 , No. 8 , pp. 2433- 2442, 2008.
20. Rahmat Allah Hooshmand and Mostafa Ezatabadi Pour, "Corrective action planning considering FACTS allocation and optimal load shedding using bacterial foraging oriented by particle swarm optimization algorithm," Turkey Journal of Electrical Engineering & Computer Science, Vol.18, No.4, pp. 597-612, 2010.
21. M. Tripathy and S. Mishra, "Bacteria Foraging-based Solution to optimize both real power loss and voltage stability limit," IEEE Transactions on Power Systems, Vol. 22, No. 1, pp. 240-248, 2007.
22. Panigrahi B.K. and Pandi V.R., "Congestion management using adaptive bacterial foraging algorithm", Energy Conversion and Management, Vol. 50, No.5, pp. 1202-1209, 2009.